



UNIVERSITY
OF TRENTO

DIPARTIMENTO DI INGEGNERIA E SCIENZA DELL'INFORMAZIONE

38123 Povo – Trento (Italy), Via Sommarive 14
<http://www.disi.unitn.it>

SYNTHESIS OF MULTI-BEAM SUB-ARRAYED ANTENNAS
THROUGH AN EXCITATIONMATCHING STRATEGY

L. Manica, P. Rocca, G. Oliveri, and A. Massa

January 2011

Technical Report # DISI-11-104

Synthesis of Multi-Beam Sub-Arrayed Antennas through an Excitation Matching Strategy

L. Manica, P. Rocca, *Student Member, IEEE*, G. Oliveri, *Student Member, IEEE*, and A. Massa,
Member, IEEE

ELEDIA Research Group

Department of Information Engineering and Computer Science,

University of Trento, Via Sommarive 14, 38050 Trento - Italy

Tel. +39 0461 882057, Fax +39 0461 882093

E-mail: *andrea.massa@ing.unitn.it*,

{luca.manica, giacomo.oliveri, paolo.rocca}@disi.unitn.it

Web: *http://www.eledia.ing.unitn.it*

Synthesis of Multi-Beam Sub-Arrayed Antennas through an Excitation Matching Strategy

L. Manica, P. Rocca, G. Oliveri, and A. Massa

Abstract

This paper presents an innovative synthesis procedure to design sub-arrayed antennas affording multiple patterns. The approach is based on an excitation matching procedure aimed at generating one optimal pattern and multiple compromises close as much as possible to user-defined reference beams. A suitable modification of the K -means clustering algorithm integrated into a customized version of the contiguous partition method is used to efficiently sample the solution space looking for the best compromise excitations. A set of representative numerical results is reported to give some indications on the reliability, potentialities, and limitations of the proposed approach.

Key words: Linear Arrays, Multi-Beam Antennas, Sub-arraying.

1 Introduction

The synthesis of switchable multi-beam antennas has always received a great attention from the scientific community because of the wide range of applications. Multi-beam antennas constitute the radiating part of monopulse radar trackers [1] to determine the positions of moving targets from the information collected by two different patterns (i.e., a sum pattern and a difference one). Furthermore, cellular base stations and communication satellites are also equipped with antennas generating multiple radiation patterns [2][3].

Multiple beams can be generated by means of reflector antennas equipped with multiple feeds or using arrays of radiating elements. Nowadays, the latter solution is preferred since it allows the direct control of the illumination on the aperture, the electronic steering of the patterns as well as the lower costs.

Several analytical methods have been developed to determine element excitations able to generate optimal sum patterns [4][5][6], difference patterns [7][8], and patterns with arbitrary shapes [9][10]. Unfortunately, the synthesis of a switchable antenna affording multiple optimal patterns implies the use of different and independent feeding networks. The total beamforming network (BFN) is usually characterized by a complex layout with a large number of active elements and high implementation costs. It is often more convenient to define compromise solutions with suitable trade-offs between costs and radiation performances. In this framework, *a-priori* fixed excitation amplitudes and optimized phase distributions for the generation of each pattern [11][12][13] as well as partially-shared apertures [14] have been considered. Another alternative is the use of sub-arrayed antennas [15]. The elements of the array are grouped into clusters which are properly weighted to generate “best” compromise patterns. The price to pay for the simplification of BFN is an unavoidable reduction of the pattern performances [16] to be limited thanks to a careful design of the sub-arrayed network and an optimization of the sub-array weights. Different synthesis approaches have been proposed to generate a single compromise beam pattern [17][18][19] and the design of sum and difference patterns has been dealt with [20][21][22][23][24][25][26], as well. In this latter, one pattern (typically the sum pattern) is generated by means of optimal excitations analytically-computed, while the difference beam is obtained throughout the sub-arrayed BFN . As regards sum-difference compromises, excitation matching strategies [20][25], approaches based on evolutionary algorithms

[21][22][23][26], and hybrid techniques [24][27] have been used.

Of course, the sub-arraying strategy can be also extended to the synthesis of multi-beam antennas [28], but such a potential has not been yet deeply investigated. By supposing the generation of $K + 1$ patterns and exploiting the guidelines of [25], once the excitations of the *main pattern* have been set through the primary feeding network, K sub-arrayed transmission lines can be designed in a serial way [*serial approach*, Σ - Fig. 1(a)] to generate the sub-optimal beam patterns. Whether on one hand the number of active elements is reduced with respect to the complete *BFN* having $K + 1$ independent transmission lines, the antenna manufacturing could still be impracticable or very complex due to the number of circuit crossing. The use of a common sub-array feed network can further simplify the complexity of the antenna design [*parallel approach*, Π - Fig. 1(b)].

This paper deals with a synthesis method based on the parallel approach for the design of multi-beam antennas. More specifically, K patterns are generated throughout a compromise *BFN* composed by a common sub-array, whereas the sub-array weights are independently computed for each beam. Likewise [25], the solution of the problem at hand is formulated as the definition of K compromise patterns close as much as possible to K reference beams by means of an excitation matching strategy.

The paper is organized as follows. In Section 2, the problem is mathematically formulated and the adopted metric as well as the solution searching procedure are presented. The results of a set of representative experiments are reported in Sect. 3 to describe the synthesis process (Sect. 3.1) and to assess the effectiveness of the proposed method (Sect. 3.2). Finally, some conclusions are drawn (Sect. 4).

2 Mathematical Formulation

Let us consider a uniform linear array of N elements with inter-element distance d . In order to generate $K + 1$ different beams on the same antenna aperture, the sub-arraying technique [20] is considered. One pattern, called *main pattern*, is generated by means of a set of optimal real excitations $\underline{A} = \{\alpha_n; n = 1, \dots, N\}$. The other K *compromise patterns* are obtained by aggregating the array elements into Q sub-arrays and assigning K weights to each of them [Fig. 1(b)]. The K sets of compromise real excitations $\underline{B}^{(k)} = \{b_n^{(k)}; n = 1, \dots, N\}$, $k = 1, \dots, K$,

are given by

$$\underline{B}^{(k)} = \{b_n^{(k)} = \delta_{c_n q} w_q^{(k)} \alpha_n; n = 1, \dots, N; q = 1, \dots, Q\}; k = 1, \dots, K, \quad (1)$$

where $c_n \in [1, Q]$ is an integer index that identifies the sub-array membership of the n -th array element to the q -th sub-array. The whole sub-array configuration is mathematically described through the vector $\underline{C} = \{c_n; n = 1, \dots, N\}$ [23]. Moreover, $w_q^{(k)}$ is the weight coefficient of the q -th sub-array related to the k -th beam and $\delta_{c_n q}$ is the Kronecker delta function ($\delta_{c_n q} = 1$ if $c_n = q$, $\delta_{c_n q} = 0$ otherwise) [25].

Following the guidelines of the optimal matching approach presented in [25] and here properly customized to the generation of multiple patterns, the problem is recast as the definition of the sub-array aggregation, \underline{C}^{opt} , and of K sets of sub-array weights, $\underline{W}_{opt}^{(k)} = \{w_q^{(k)}; q = 1, \dots, Q\}$, $k = 1, \dots, K$, that minimize the least square distance between the compromise excitations, $\underline{B}^{(k)}$, $k = 1, \dots, K$, and the reference ones, $\underline{B}_{ref}^{(k)} = \{\beta_n^{(k)}; n = 1, \dots, N\}$, $k = 1, \dots, K$. The cost function that quantifies such a mismatch is given by

$$\Psi(\underline{C}_i, \underline{\underline{W}}_i) = \max_{k=1, \dots, K} \left\{ \Psi^{(k)}(\underline{C}_i, \underline{W}_i^{(k)}) \right\}, \quad (2)$$

where $\underline{\underline{W}}_i = \{\underline{W}_i^{(k)}; k = 1, \dots, K\}$ and

$$\Psi^{(k)}(\underline{C}_i, \underline{W}_i^{(k)}) = \frac{1}{N} \sum_{n=1}^N \left[\beta_n^{(k)} - b_n^{(k)}(\underline{C}_i, \underline{W}_i^{(k)}) \right]^2. \quad (3)$$

By substituting (1) into (3) and after simple mathematical manipulations, it turns out that

$$\Psi^{(k)}(\underline{C}_i, \underline{W}_i^{(k)}) = \frac{1}{N} \sum_{n=1}^N \alpha_n^2 \left[\frac{\beta_n^{(k)}}{\alpha_n} - \sum_{q=1}^Q \delta_{c_n q} w_q^{(k)}(\underline{C}_i, \underline{W}_i^{(k)}) \right]^2. \quad (4)$$

As shown in [25], once the sub-array configuration \underline{C}_i is set, the weights $\underline{W}_i^{(k)} = \{w_q^{(k)}; q = 1, \dots, Q\}$, $k = 1, \dots, K$, are defined as follows

$$w_q^{(k)} = \frac{\sum_{q=1}^Q \sum_{n=1}^N \delta_{c_n q} \alpha_n^2 v_n^{(k)}}{\sum_{q=1}^Q \sum_{n=1}^N \delta_{c_n q} \alpha_n^2}, \quad q = 1, \dots, Q, \quad k = 1, \dots, K. \quad (5)$$

where $v_n^{(k)} = \frac{\beta_n^{(k)}}{\alpha_n}$, $n = 1, \dots, N$, are the *reference weights* [25], namely those coefficients generating K optimal patterns when using independent *BFNs*.

In order to optimize (2), let us first define N *reference vectors*, $\underline{V}_n \in \mathbb{R}^K$, $n = 1, \dots, N$, as

$$\underline{V}_n = \{v_n^{(k)}; k = 1, \dots, K\}; \quad n = 1, \dots, N. \quad (6)$$

Unlike [25], where the Contiguous Partition Method (*CPM*) has been proposed to synthesize one compromise pattern ($K = 1$), we are now aimed at extending the *CPM* to deal with K sub-optimal patterns ($K - CPM$). Unfortunately, the guidelines of [29] suitably exploited in [25] cannot be applied here since a sorting property for the reference vectors \underline{V}_n , $n = 1, \dots, N$ does not exist. However, it is still expected that \underline{C}^{opt} is the result of the aggregation within the same sub-array of those elements whose reference vectors are close in \mathbb{R}^K . Accordingly, the problem at hand is then reformulated as “*searching the best grouping \underline{C}^{opt} for assigning N vector points to Q disjoint sub-sets \underline{S}_q , $q = 1, \dots, Q$ ($Q < N$) such that the internal variances of the subsets, computed as (4), are minima*”. State-of-the-art literature refers this problem as the unsupervised clustering problem [30]. Several techniques have been proposed to deal with it and the *K-means* (here referred as *Q-means*) *Clustering Algorithm* [31][32] is chosen hereinafter because of the convergence rate and the simplicity of implementation.

In order to look for the “best” compromise solution, the proposed algorithm works as follows:

- **Step 0 - Initial Step**

Reference Excitations Selection - The excitations of the *main pattern*, \underline{A} , as well as the reference excitations of the compromise beams, $\underline{B}_{ref}^{(k)}$, $k = 1, \dots, K$ are chosen;

Initialization - The reference vectors, \underline{V}_n , $n = 1, \dots, N$, [Fig. 2(a)] are computed and the iteration counter is initialized ($i = 0$). If the elements $v_n^{(k)}$ are not positive, they are translated of the quantity

$$\gamma^{(k)} = \min_{n=1, \dots, N} \{v_n^{(k)}\} \quad (7)$$

to obtain the set of translated reference vectors $\widehat{\underline{V}}_n = \underline{V}_n - \underline{\Gamma}$, $n = 1, \dots, N$, where $\underline{\Gamma} = \{\gamma^{(k)}; k = 1, \dots, K\}$ [Fig. 2(b)]. Successively, the norms of the vectors $\widehat{\underline{V}}_n$, $n = 1, \dots, N$, are computed

$$r_n = \sqrt{\sum_{k=1}^K [\hat{v}_n^{(k)}]^2}; \quad n = 1, \dots, N \quad (8)$$

and their values are sorted on a line [Fig. 2(c)] to determine the list L

$$L = \left\{ l_j; j = 1, \dots, N; l_j \leq l_{j+1}; l_1 = \widehat{\underline{V}}_n \mid r_n = \min_{n=1, \dots, N} (r_n); l_N = \widehat{\underline{V}}_n \mid r_n = \max_{n=1, \dots, N} (r_n) \right\}. \quad (9)$$

The initial sub-array configuration \underline{C}_0 is obtained by randomly choosing $Q - 1$ cut points among the $N - 1$ inter-element spaces of the list L [Fig. 2(d)], then defining the initial subsets $\underline{S}_q^{(0)} = \{\widehat{\underline{V}}_{n_q}^{(0)}; n_q = 1, \dots, N_q^{(0)}\}$, $q = 1, \dots, Q$, being $N = \sum_{q=1}^Q N_q^{(0)}$. Moreover, the Euclidean distance between each couple of reference vectors is computed

$$d(\widehat{\underline{V}}_n, \widehat{\underline{V}}_p) = \sqrt{\sum_{k=1}^K [\hat{v}_n^{(k)} - \hat{v}_p^{(k)}]^2}, \quad n = 1, \dots, N - 1; p = n + 1, \dots, N. \quad (10)$$

The sequence index is set to $j = 1$;

- **Step 1 - Cost Function Evaluation** - The cost function of the current aggregation $\underline{C}_{i(j)}$ is evaluated by means of (3), $\Psi_{i(j)} = \Psi(\underline{C}_{i(j)}, \underline{W}_{i(j)})$, and compared with the best cost function value obtained up-till now, $\Psi_{i-1}^{opt} = \min_{h=1, \dots, i-1} \{\Psi(\underline{C}_h, \underline{W}_h)\}$. If $\Psi_{i(j)} < \Psi_{i-1}^{opt}$ then the optimal cost function is updated ($\Psi_i^{opt} = \Psi_{i(j)}$) by also setting $\underline{C}_i^{opt} = \underline{C}_{i(j)}$, elsewhere $\Psi_i^{opt} = \Psi_{i-1}^{opt}$;
- **Step 2 - Convergence Check** - If $i \geq I_{max}$ (I_{max} being the maximum number of iterations) or the solution is stationary for Z_{max} iterations (i.e., $\Psi_i = \Psi_{i-z}$, $z = 1, \dots, Z_{max}$), then the optimization process is stopped;
- **Step 3 - Sequence Updating** - The sequence index is updated ($j \leftarrow j + 1$) and if $j \leq N$ then the process jumps to Step 5;
- **Step 4 - Iteration Updating** - The iteration index is updated ($i \leftarrow i + 1$) and the sequence index is reset ($j = 1$);

- **Step 5 - Border Element Identification** - The vector $\widehat{\underline{V}}_n$ related to the list element l_j is selected. It is a *border vector*, $\widetilde{\underline{V}}_n$, if

$$d\left(\widehat{\underline{V}}_n, \underline{\Omega}\right) < \min_{\widehat{\underline{V}}_p \in \underline{S}_q^{i(j)}; p=1, \dots, N_q^{i(j)}; p \neq n} \left[d\left(\widehat{\underline{V}}_n, \widehat{\underline{V}}_p\right) \right], \quad \widehat{\underline{V}}_n \in \underline{S}_q^{i(j)} \quad (11)$$

where $\underline{\Omega}$ is the reference vector given by

$$\underline{\Omega} = \arg \left\{ \min_{\widehat{\underline{V}}_p \notin \underline{S}_q^{i(j)}; p=1, \dots, N; q=1, \dots, Q} \left[d\left(\widehat{\underline{V}}_n, \widehat{\underline{V}}_p\right) \right] \right\}. \quad (12)$$

and belonging to the subset $\underline{S}_\Omega^{i(j)}$, $\Omega \in [1, Q]$. If (11) holds true then the algorithm goes to Step 6. Otherwise, the Step 3 is repeated;

- **Step 6 - Aggregation Updating** - The border element $\widetilde{\underline{V}}_n$ is aggregated to the subset $\underline{S}_\Omega^{i(j)}$ (and to the corresponding sub-array) to obtain a new trial configuration $\underline{C}_{i(j)}$. If $\Psi\left(\underline{C}_{i(j)}\right) < \Psi\left(\underline{C}_i\right)$, then $\underline{C}_i = \underline{C}_{i(j)}$ (i.e., $\underline{S}_q^i = \underline{S}_q^{i(j)}$, $q = 1, \dots, Q$) and the Step 1 is iterated. Otherwise, the algorithm goes to Step 3.

3 Numerical Results

In this section, the results of representative simulations are reported to show the behavior of the $K - CPM$ synthesis process as well as the performances of the proposed approach. In order to provide quantitative information, the mainlobe beamwidth, BW , the position of the first pattern null, θ_0 , and the peak sidelobe level, SLL , have been evaluated for the compromise patterns and compared to those of the reference ones. Furthermore, the *matching indexes* [25]

$$\Delta^{(k)} = \frac{\int_{-\pi/2}^{\pi/2} \left| \left| AF_{ref}^{(k)}(\theta) \right| - \left| AF_{rec}^{(k)}(\theta) \right| \right| d\theta}{\int_{-\pi/2}^{\pi/2} \left| AF_{ref}^{(k)}(\theta) \right| d\theta} \quad k = 1, \dots, K \quad (13)$$

have been used to quantify the degree of matching with references. In (13), $\left| AF_{ref}^{(k)}(\theta) \right|$ and $\left| AF_{rec}^{(k)}(\theta) \right|$ are the normalized k -th reference array pattern and that synthesized with the proposed approach, respectively. For comparative purposes, the solution synthesized with the serial implementation of the $K - CPM$ is given, as well.

Let us consider a linear array of $N = 2 \times M = 20$ elements with $d = \frac{\lambda}{2}$ and the generation

of three beams ($K = 2$). The main pattern excitations $\underline{A} = \{\alpha_m = \alpha_{-m}; m = 1, \dots, M\}$ have been set to those of a Dolph-Chebyshev pattern [4] with $SLL = -25 \text{ dB}$, while the reference coefficients for the first compromise pattern, $\underline{B}_{ref}^{(1)} = \{\beta_m^{(1)} = -\beta_{-m}^{(1)}; m = 1, \dots, M\}$, and the second one, $\underline{B}_{ref}^{(2)} = \{\beta_m^{(2)} = \beta_{-m}^{(2)}; m = 1, \dots, M\}$, have been chosen to afford a Zolotarev difference pattern [8] with $SLL = -30 \text{ dB}$ and a Taylor sum pattern [6] with $SLL = -25 \text{ dB}$ and $\bar{n} = 4$, respectively. The number of sub-arrays has been chosen equal to $Q = 3$. By virtue of the symmetries among the excitation coefficients, only half array has been involved in the synthesis process ($m = 1, \dots, M$).

At the first step of the parallel $K - CPM$, the reference vectors (6) are computed. Since all the $v_m^{(k)}$ terms are positive, it follows that $\widehat{\underline{V}}_m = \underline{V}_m$. The values of the reference vectors and their norms (8) are reported in Tab. I. Starting from the initial randomly-chosen configuration equal to $\underline{C}_0 = \{2, 2, 3, 3, 3, 3, 3, 3, 3, 1\}$, the clustering is iteratively updated. The evolution of the sub-array aggregations is shown in Fig. 3 [$i = 0$ - Fig. 3(a); $i = 1$ - Fig. 3(b); $i = 3$ - Fig. 3(c) and $i = 10$ - Fig. 3(d)]. The corresponding patterns are reported in Fig. 4 ($k = 1$ - left column; $k = K = 2$ - right column). It is worth noting that the initial aggregation leads to a compromise difference far from the target [Fig. 4(a)], whereas the second beam is close to the corresponding reference [Fig. 4(b)]. Such a situation is confirmed by the values of the cost function $\Psi_0^{(1)} = 2.05 \times 10^{-1}$ and $\Psi_0^{(2)} = 2.02 \times 10^{-4}$ in Fig. 5. At the convergence ($i = i_{opt}$), the trade-off solution shows in Figs. 4(g)-4(h) is obtained. The synthesized patterns identified by the label “II” are shown in Fig. 6(a) ($k = 1$) and Fig. 6(c) ($k = 2$) along with the solution from the serial implementation of the CPM (line “Σ”). The corresponding HW layouts are also given in Figs. 6(b) and 6(d), as well. For completeness, the sub-array configurations and weights are listed in Tab. II, whereas the values of the pattern indexes are reported in Tab. III. As it can be observed, both implementations do not exactly match the reference difference [Fig. 6(a) - Tab. III (*Pattern I*)], while a good fitting is achieved in correspondence with the pattern $k = 2$. Moreover, the same compromise difference beam ($k = 1$) is generated by the two $K - CPM$ architectures, while the pattern matching for the sum beam [Fig. 6(c)] slightly worsens with the parallel solution against a significant reduction of the circuit complexity ($C_\Sigma = 56$ vs. $C_{II} = 16$, C being the crossing count).

In order to assess the reliability of the proposed strategy, Figure 7 gives some indications on

the asymptotic behavior of the method performances. More specifically, the values of $\Psi^{(1)}$ and $\Psi^{(2)}$ [Fig. 7(a)] and of the indexes $\Delta^{(1)}$ and $\Delta^{(2)}$ [Fig. 7(b)] versus Q are reported for both implementations. As expected, the plots present a monotonic decreasing behavior and $\Delta^{(k)} \rightarrow 0$ when $Q \rightarrow M$.

The second example (*Test 2*) deals with the synthesis of a linear array with $N = 2 \times M = 12$ elements ($d = \frac{\lambda}{2}$) generating a flat-topped main beam and two compromise patterns. The flat-topped pattern is characterized by ripples within the main lobe region of amplitude ± 0.5 dB and $SLL = -20$ dB. It is afforded by a set of symmetrical real excitations available in [9]. The reference excitations for the first and the second sub-arrayed beams have been chosen to generate a Zolotarev pattern [8] with $SLL = -25$ dB and a Dolph-Chebyshev pattern [4] with $SLL = -25$ dB. The reference excitations are given in Tab. IV (rows 2-4). The number of sub-arrays has been set to $Q = 4$.

The final aggregations and the corresponding weights synthesized with the proposed parallel $K - CPM$ approach are $\underline{C}^{opt} = \{3, 4, 1, 2, 3, 4\}$, $\underline{W}^{(1)} = \{-13.29, -4.73, 0.28, 1.80\}$, and $\underline{W}^{(2)} = \{-10.30, -3.15, 1.00, 2.09\}$, respectively. In this case, the same result is obtained by the serial approach as confirmed by the value of the cost function as well as from the matching indexes (Tab. V). The convergence patterns are shown in Fig. 8 along with the HW layouts of both architectures ($C_{\Sigma} = 39$ vs. $C_{\Pi} = 12$). As far as the pattern performance are concerned (Tab. V), the sum pattern presents a $SLL = -19.46$ dB of almost 5 dB above the value of the reference beam. Moreover, $BW = 9.29$ [deg] vs. $BW^{ref} = 8.26$ [deg]. A better matching has been yielded for the difference pattern since $SLL = -22.27$ dB vs. $SLL^{ref} = -24.76$ dB and $BW = 9.97$ [deg] vs. $BW^{ref} = 10.57$ [deg].

The last test case (*Test 3*) is concerned with the synthesis of a large linear array having $N = 2 \times M = 100$ elements ($d = \frac{\lambda}{2}$) with a compromise feed network of $Q = 8$ sub-arrays. The main pattern has been set to a Taylor pattern with $SLL = -35$ dB and $\bar{n} = 6$ [6]. Two reference difference patterns have been chosen, namely a modified Zolotarev pattern with $SLL = -30$ dB and $\bar{n} = 5$ [33] and a difference pattern providing maximum directivity whose excitations have been computed as proposed in [34].

The sub-array configuration and the corresponding weights synthesized with the $K - CPM$ approaches are reported in Tab. VI. A pictorial representation in the reference vector space of

the element aggregation is shown in Fig. 9. As expected, the searching procedure is able to aggregate in the same sub-array the array elements whose reference vectors are closer. In Fig. 10, the patterns radiated by the parallel $K - CPM$ solution are shown. For the sake of clarity, only the envelopes are plotted.

Figure 11 compares the $K - CPM$ patterns with the reference ones in correspondence with $k = 1$ [Fig. 11(a)] and $k = 2$ [Fig. 11(b)], respectively. As it can be observed, the parallel solution gets worse than the serial implementation dealing with the difference pattern ($k = 1$ - Tab. VII) when the matching with the reference one is also not very accurate [Fig. 11(a)] especially outside the angular region close to the mainlobe (i.e., $\theta \geq 10^\circ$). On the other hand, it is worthwhile to notice the strong reduction of the layout complexity obtained with the parallel architecture since $C_\Sigma = 150$ vs. $C_\Pi = 50$. As regards $k = 2$ [Fig. 11(b)], both $K - CPM$ patterns have the same pattern features of the reference beam (i.e., $SLL = -12.71$ dB and $BW = 0.87$ [deg]) even though the maximum directivity slightly reduces ($D_{max}^{ref} = 17.84$ dB vs. $D_{max} = 17.79$ dB).

As far as the computational burden is concerned, Table VIII summarizes the main issues: U (dimension of the solution space), i_{opt} (number of iterations), ψ_{opt} (number of cost function evaluations), and T (CPU time). Despite the wide dimension of the solution space with $U \simeq 1.43 \times 10^{45}$ admissible alternatives, the process for defining the Π layout takes just $i_{opt} = 6$ iterations and it requires $\psi_{opt} = 258$ cost function evaluations performed in only $T = 0.86$ [sec]. In such a case, the extra computation time with respect to the serial implementation ($\frac{T_\Pi}{T_\Sigma} \simeq 5.6$) is mainly related to the sorting process of the reference vectors.

4 Conclusions

In this paper, an innovative approach for the synthesis of multiple-beam sub-arrayed antennas has been presented. The solution procedure is based on an excitation matching algorithm aimed at defining an optimal pattern through a set of independent excitations and synthesizing multiple compromise beams by using a common sub-array feed network and independent sub-array weights for each pattern. A fast searching procedure exploiting a suitable integration of the CPM with a customized version of the K -means clustering algorithm has been used to effectively sample the space of admissible solutions. The obtained results have proved the feasibility

of the proposed method as well as its reliability in fitting multiple reference patterns with satisfactory performances and a limited circuit complexity. The computational efficiency of the approach has been pointed out dealing with large linear arrays, as well.

References

- [1] I. M. Skolnik, *Radar Handbook* (3rd Ed.). McGraw-Hill, 2008.
- [2] C. A. Balanis, *Antenna Theory: Analysis and Design* (3rd Ed.). Wiley, 2005.
- [3] M. Barba, J. E. Page, J. A. Encinar, and J. R. Montejo-Garai, "A switchable multiple beam antenna for GSM-UMTS base stations in planar technology," *IEEE Trans. Antennas Propag.*, vol. 54, no. 11, pp. 3087-3094, Nov. 2006.
- [4] C. L. Dolph, "A current distribution for broadside arrays which optimises the relationship between beam width and sidelobe level," *Proc. IRE*, vol. 34, pp. 335-348, 1946.
- [5] T. T. Taylor, "Design of line-source antennas for narrow beam-width and low side lobes," *Trans. IRE*, vol. AP-3, pp. 16-28, 1955.
- [6] A. T. Villeneuve, "Taylor pattern for discrete arrays," *IEEE Trans. Antennas Propag.*, vol. AP-32, no. 10, pp. 1089-1093, Oct. 1984.
- [7] E. T. Bayliss, "Design of monopulse antenna difference patterns with low sidelobes," *Bell System Tech. Journal*, vol. 47, pp. 623-640, 1968.
- [8] D. A. McNamara, "Direct synthesis of optimum difference patterns for discrete linear arrays using Zolotarev distribution," *IEE Proc. H Microw. Antennas Propag.*, vol. 140, no. 6, pp 445-450, Dec. 1993.
- [9] Y. U. Kim and R. S. Elliott, "Shaped-pattern synthesis using pure real distributions," *IEEE Trans. Antennas Propag.*, vol. 36, no. 11, pp. 1645-1649, Nov. 1988.
- [10] F. Ares, R. S. Elliott, and E. Moreno "Synthesis of shaped line-source antenna beams using pure real distributions," *Electron. Lett.*, vol. 30, no. 4, pp. 280-281, Feb. 1994.

- [11] M. Durr, A. Trastoy, and F. Ares, "Multiple-pattern linear antenna arrays with single prefixed amplitude distributions: modified Woodward-Lawson synthesis," *Electron. Lett.*, vol. 36, no. 16, pp. 1345-1346, Aug. 2000.
- [12] A. Trastoy, Y. Rahmat-Samii, F. Ares, and E. Moreno, "Two-pattern linear array antenna: synthesis and analysis of tolerance," *IEE Proc. Microw. Antennas Propag.*, vol. 151, no. 2, pp. 127-130, Apr. 2004.
- [13] M. Comisso and R. Vescovo, "Multi-beam synthesis with null constraints by phase control for antenna arrays of arbitrary geometry," *Electron. Lett.*, vol. 43, no. 7, pp. 374-375, Mar. 2007.
- [14] M. Alvarez, J. A. Rodriguez, and F. Ares, "Synthesising Taylor and Bayliss linear distributions with common aperture tail," *Electron. Lett.*, vol. 45, no. 1, pp. 18-19, Jan. 2009.
- [15] R. J. Mailloux, *Phased array antenna handbook*. Artech House, Boston, MA, 2005.
- [16] R. J. Mailloux, "Phased array theory and technology," *IEEE Proc.*, vol. 70, no. 3, pp. 246-302, Mar. 1982.
- [17] K. S. Rao and I. Karlsson, "Low sidelobe design considerations of large linear array antennas with contiguous subarrays," *IEEE Trans. Antennas Propag.*, vol. 35, no. 4, pp. 361-366, Apr. 1987.
- [18] N. Toyama, "Aperiodic array consisting of subarrays for use in small mobile earth stations," *IEEE Trans. Antennas Propag.*, vol. 53, no. 6, pp. 2004-2010, Jun. 2005.
- [19] R. L. Haupt, "Optimized weighting of uniform subarrays of unequal size," *IEEE Trans. Antennas Propag.*, vol. 55, no. 4, pp. 1207-1210, Apr. 2007.
- [20] D. A. McNamara, "Synthesis of sub-arrayed monopulse linear arrays through matching of independently optimum sum and difference excitations," *IEE Proc. H Microw. Antennas Propag.*, vol. 135, no. 5, pp. 371-374, 1988.
- [21] F. Ares, S. R. Rengarajan, J. A. Rodriguez, and E. Moreno, "Optimal compromise among sum and difference patterns," *J. Electromag. Waves Appl.*, vol. 10, pp. 1143-1555, 1996.

- [22] P. Lopez, J. A. Rodriguez, F. Ares, and E. Moreno, "Subarray weighting for difference patterns of monopulse antennas: joint optimization of subarray configurations and weights," *IEEE Trans. Antennas Propag.*, vol. 49, no. 11, pp. 1606-1608, Nov. 2001.
- [23] S. Caorsi, A. Massa, M. Pastorino, and A. Randazzo, "Optimization of the difference patterns for monopulse antennas by a hybrid real/integer-coded differential evolution method," *IEEE Trans. Antennas Propag.*, vol. 53, no. 1, pp. 372-376, Jan. 2005.
- [24] M. D'Urso, T. Isernia, and E. F. Meliadò, "An effective hybrid approach for the optimal synthesis of monopulse antennas," *IEEE Trans. Antennas Propag.*, vol. 55, no. 4, pp. 1059-1066, Apr. 2007.
- [25] L. Manica, P. Rocca, A. Martini, and A. Massa, "An innovative approach based on a tree-searching algorithm for the optimal matching of independently optimum sum and difference excitations," *IEEE Trans. Antennas Propag.*, vol. 56, no. 1, pp. 58-66, Jan. 2008.
- [26] Y. Chen, S. Yang, and Z. Nie, "The application of a modified differential evolution strategy to some array pattern synthesis problems," *IEEE Trans. Antennas Propag.*, vol. 56, no. 7, pp. 1919-1927, Jul. 2008.
- [27] P. Rocca, L. Manica, R. Azaro, and A. Massa, "A hybrid approach to the synthesis of subarrayed monopulse linear arrays," *IEEE Trans. Antennas Propag.*, vol. 57, no. 1, pp. 280-283, Jan. 2009.
- [28] W. Wen-Chang, L. Chun-Jing, L. Feng, and Li Lei, "A new multi-beam forming method for large array," *Proc. IEEE Radar Conf. 2009*, Pasadena, CA (USA), 4-8 May 2009, pp. 1-4.
- [29] W. D. Fisher, "On grouping for maximum homogeneity," *American Statistical Journal*, 789-798, 1958.
- [30] R. O. Duda, P. E. Hart, and D. G. Stork, *Pattern Classification* (2nd Ed.). Wiley, 2000.

- [31] J. B. MacQueen, "Some methods for classification and analysis of multivariate observation," *Proc. 5-th Berkley Symposium on Mathematical Statistics and Probability*, Berkeley, University of California Press, pp. 281-297, 1967.
- [32] S. P. Lloyd, "Least square quantization in PCM," *IEEE Trans. Inf. Theory*, vol. 28, no. 2, pp. 129-137, Mar. 1982.
- [33] D. A. McNamara, "Discrete \bar{n} -distribution for difference patterns," *Electron. Lett.*, vol. 22, no.6, pp. 303-304, Mar. 1986.
- [34] D. A. McNamara, "Excitations providing maximal directivity for difference arrays of discrete elements," *Electron. Lett.*, vol. 23, no. 15, pp. 780-781, Jul. 1987.

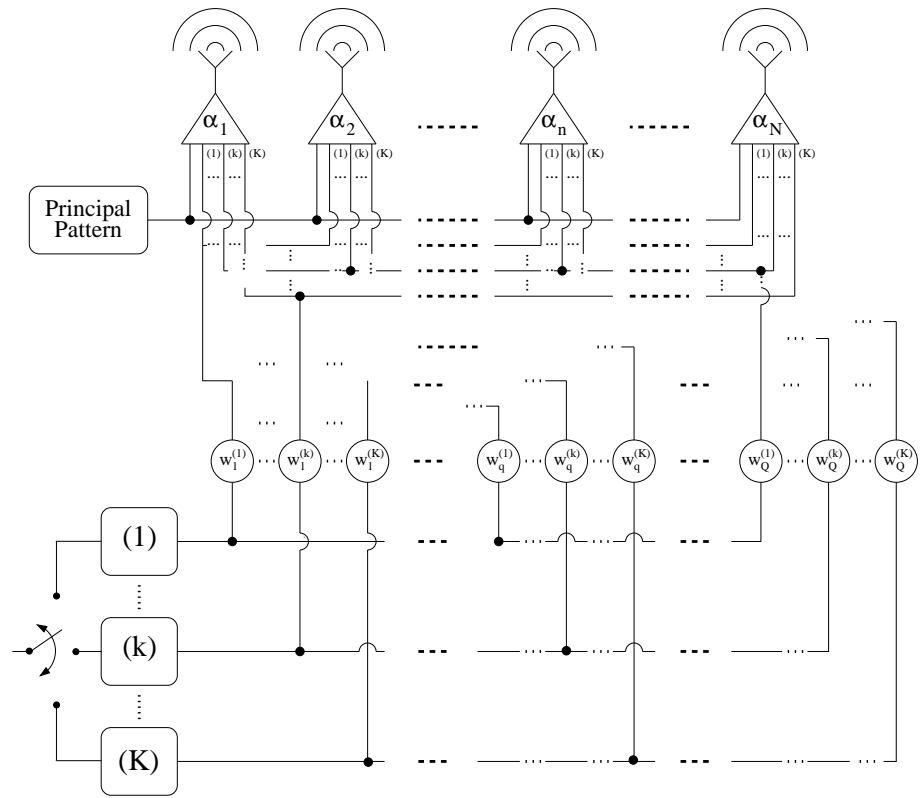
FIGURE CAPTIONS

- **Figure 1.** Sketch of the multi-beam sub-arrayed antenna: (a) serial architecture and (b) parallel architecture.
- **Figure 2.** *Parallel $K - CPM$ - Synthesis Process* ($N = 12, K = 2, Q = 3$). (a) Reference vectors $\underline{V}_n = \{v_n^{(k)}; k = 1, \dots, K\}, n = 1, \dots, N$, (b) translated reference vectors $\hat{\underline{V}}_n = \{\hat{v}_n^{(k)}; k = 1, \dots, K\}, n = 1, \dots, N$, (c) generation of the list L of the norm values of the references vectors, and (d) element aggregation and definition of the sub-array configuration, \underline{C} .
- **Figure 3.** *Parallel $K - CPM$ Analysis (Test 1: $N = 20, K = 2, Q = 3$)* - Sub-array configuration synthesized at (a) $i = 0$, (b) $i = 1$, (c) $i = 3$ and (d) $i = i_{opt} = 10$.
- **Figure 4.** *Parallel $K - CPM$ Analysis (Test 1: $N = 20, K = 2, Q = 3$)* - Relative power patterns synthesized at iteration (a)(b) $i = 0$, (c)(d) $i = 1$, (e)(f) $i = 3$ and (g)(h) $i = i_{opt} = 10$. Difference compromise pattern, $k = 1$ (left column) and sum compromise pattern, $k = 2$ (right column).
- **Figure 5.** *Parallel $K - CPM$ Analysis (Test 1: $N = 20, K = 2, Q = 3$)* - Behavior of the cost function Ψ and of the terms $\Psi^{(1)}$ and $\Psi^{(2)}$ during the iterative synthesis process (i : iteration index).
- **Figure 6.** *$K - CPM$ Multi-Beam Synthesis (Test 1: $N = 20, K = 2, Q = 3$)* - Patterns synthesized with the $K - CPM$ techniques at $k = 1$ (a) and $k = 2$ (c). Array layouts: (b) serial architecture and (d) parallel architecture.
- **Figure 7.** *$K - CPM$ Asymptotic Analysis ($N = 20, K = 2$)* - Behavior of (a) the cost function terms $\Psi^{(1)}$ and $\Psi^{(2)}$ and of (b) the matching indexes $\Delta^{(1)}$ and $\Delta^{(2)}$ versus Q ($Q = 2, \dots, 10$).
- **Figure 8.** *$K - CPM$ Multi-Beam Synthesis (Test 2: $N = 12, K = 2, Q = 4$)* - Optimal and compromise patterns (a). Layouts derived from the serial approach (b) and the parallel approach (c).

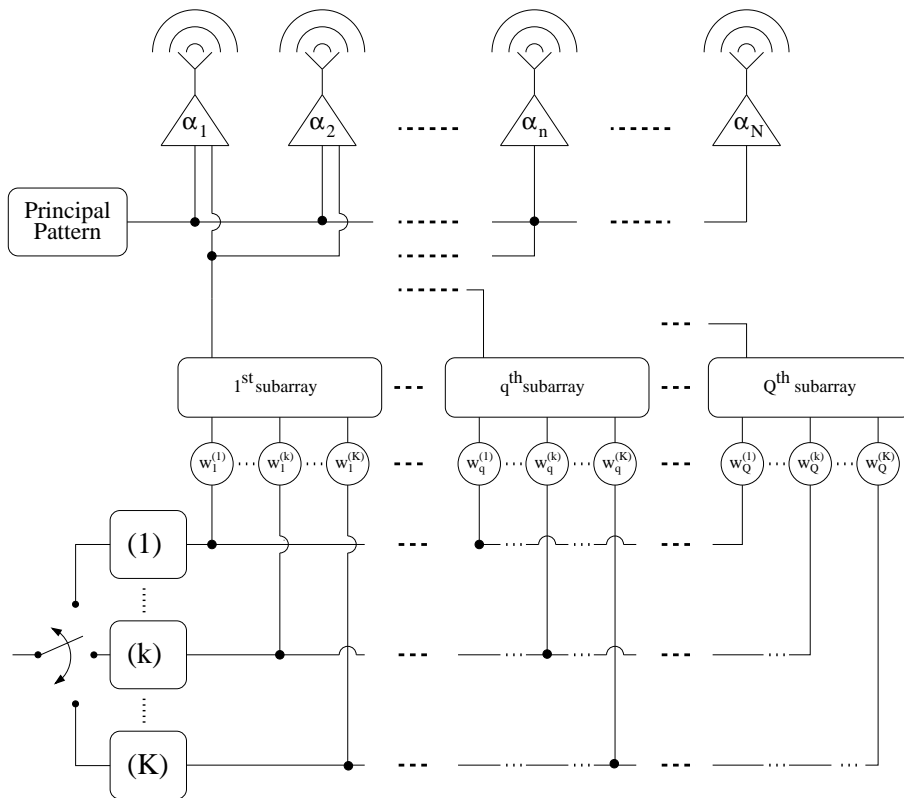
- **Figure 9.** *K – CPM Multi-Beam Synthesis (Test 3: $N = 100, K = 2, Q = 8$)* - Representation in the reference vector space of the sub-array configurations synthesized with the *K – CPM* techniques.
- **Figure 10.** *Parallel K – CPM Multi-Beam Synthesis (Test 3: $N = 100, K = 2, Q = 8$)* - Main and compromise patterns ($k = 1, 2$).
- **Figure 11.** *K – CPM Multi-Beam Synthesis (Test 3: $N = 100, K = 2, Q = 8$)* - Reference and compromise patterns synthesized with the *K – CPM* techniques: (a) $k = 1$ and (b) $k = 2$.

TABLE CAPTIONS

- **Table I.** *Parallel K – CPM Multi-Beam Synthesis (Test 1: $N = 20, K = 2, Q = 3$)* - Reference vectors and their norms.
- **Table II.** *K – CPM Multi-Beam Synthesis (Test 1: $N = 20, K = 2, Q = 3$)* - Sub-array configurations and sub-array weights.
- **Table III.** *K – CPM Multi-Beam Synthesis (Test 1: $N = 20, K = 2, Q = 3$)* - Performances indexes.
- **Table IV.** *Parallel K – CPM Multi-Beam Synthesis (Test 2: $N = 12, K = 2, Q = 4$)* - Reference excitations and reference vectors.
- **Table V.** *K – CPM Multi-Beam Synthesis (Test 2: $N = 12, K = 2, Q = 4$)* - Performances indexes.
- **Table VI.** *K – CPM Multi-Beam Synthesis (Test 3: $N = 100, K = 2, Q = 8$)* - Synthesized sub-array configurations and weights.
- **Table VII.** *K – CPM Multi-Beam Synthesis (Test 3: $N = 100, K = 2, Q = 8$)* - Performances indexes.
- **Table VIII.** *K – CPM Multi-Beam Synthesis (Test 3: $N = 100, K = 2, Q = 8$)* - Computational indexes.



(a)



(b)

Fig. 1 - L. Manica *et al.*, "Synthesis of Multi-Beam Sub-Arrayed Antennas ..."

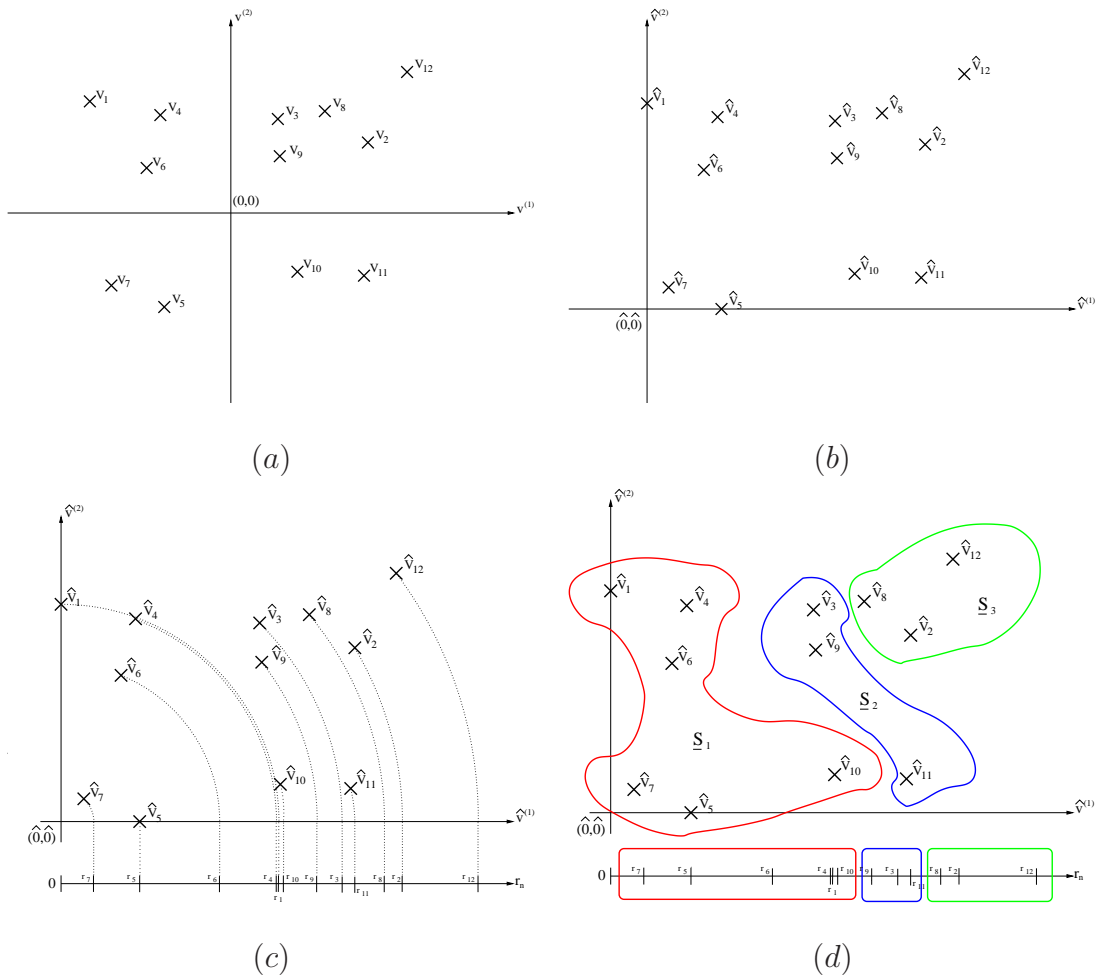
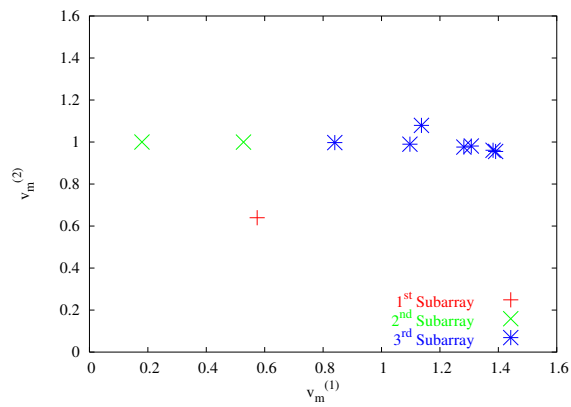
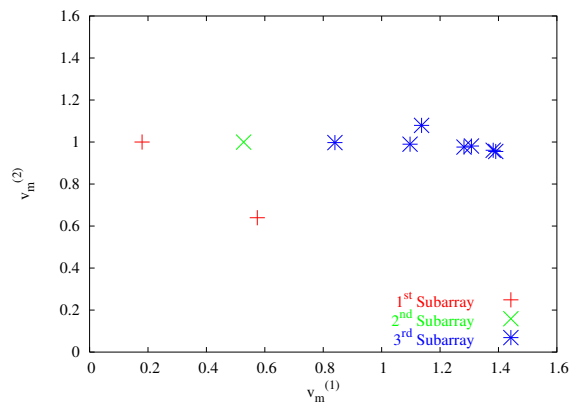


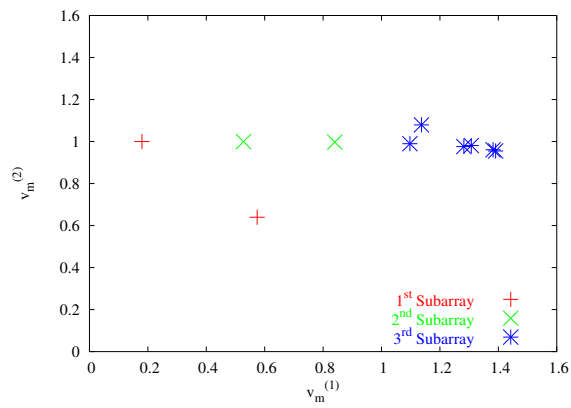
Fig. 2 - L. Manica *et al.*, “Synthesis of Multi-Beam Sub-Arrayed Antennas ...”



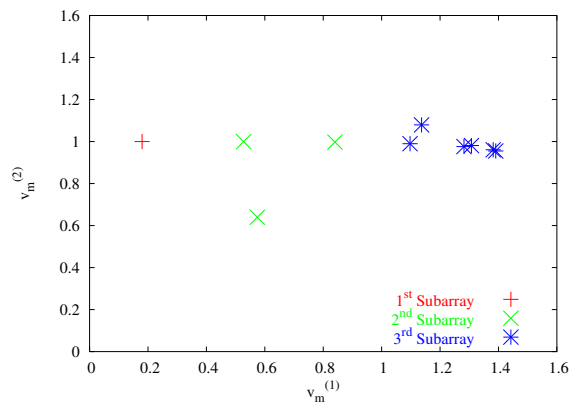
(a)



(b)

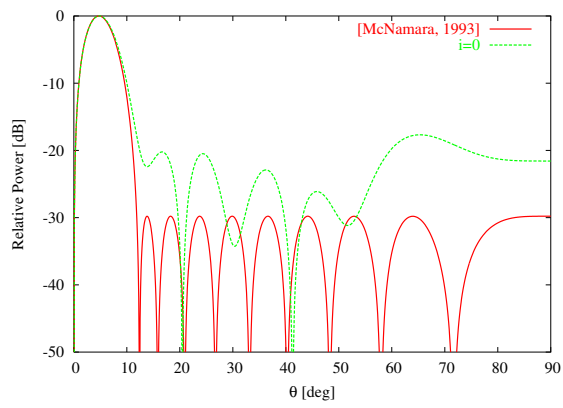


(c)

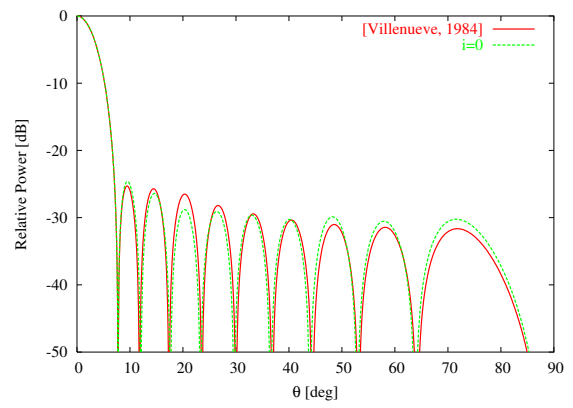


(d)

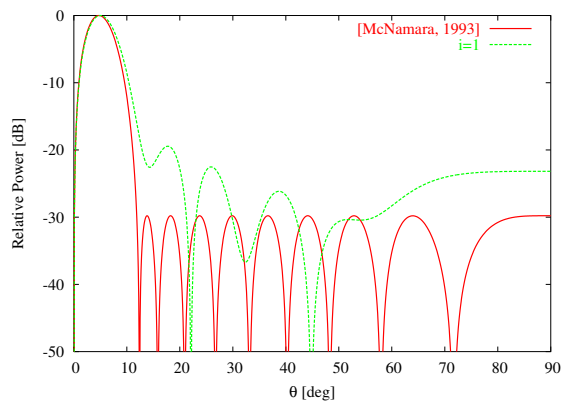
Fig. 3 - L. Manica *et al.*, “Synthesis of Multi-Beam Sub-Arrayed Antennas ...”



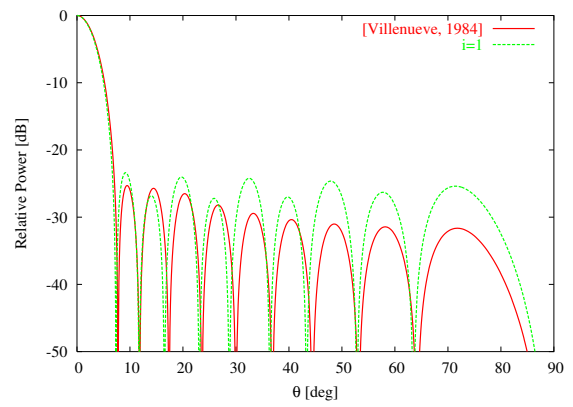
(a)



(b)

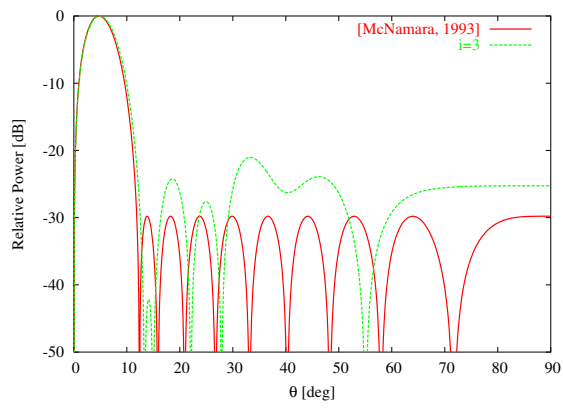


(c)

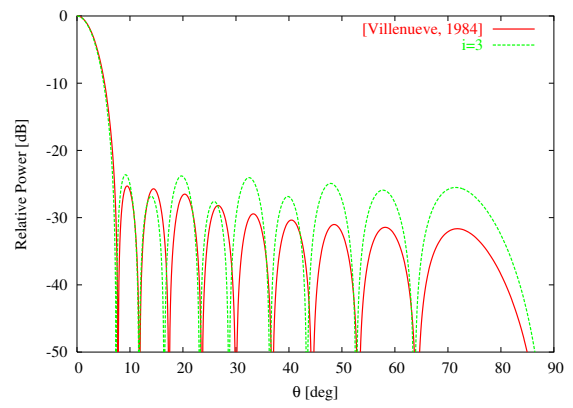


(d)

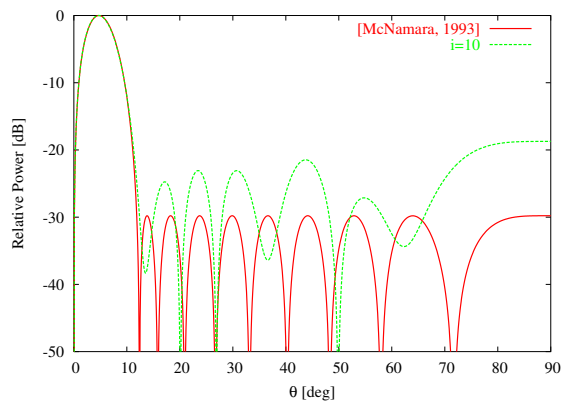
Fig. 4(I) - L. Manica *et al.*, "Synthesis of Multi-Beam Sub-Arrayed Antennas ..."



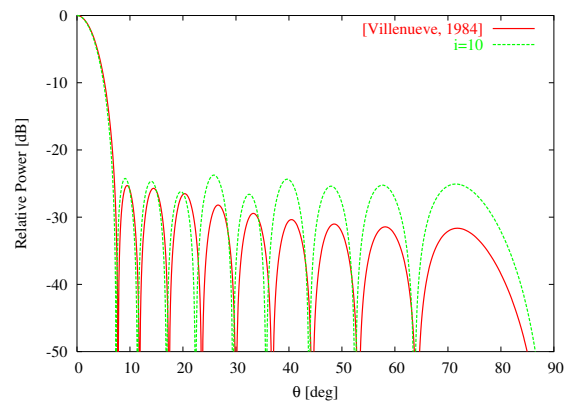
(e)



(f)



(g)



(h)

Fig. 4(II) - L. Manica *et al.*, "Synthesis of Multi-Beam Sub-Arrayed Antennas ..."

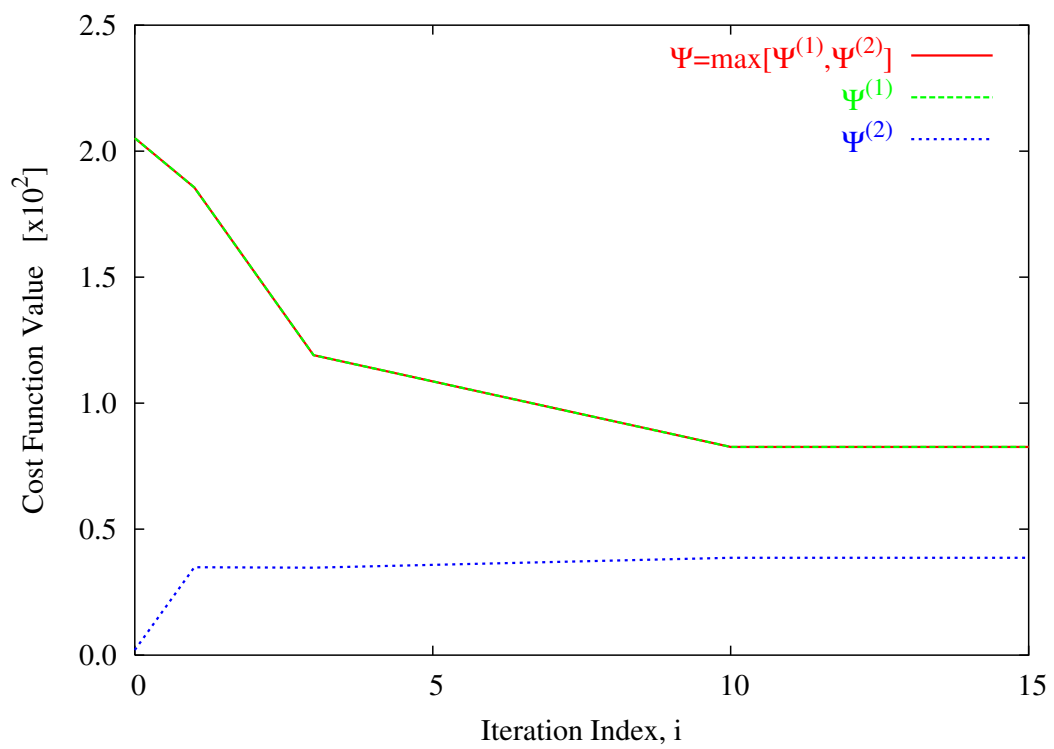
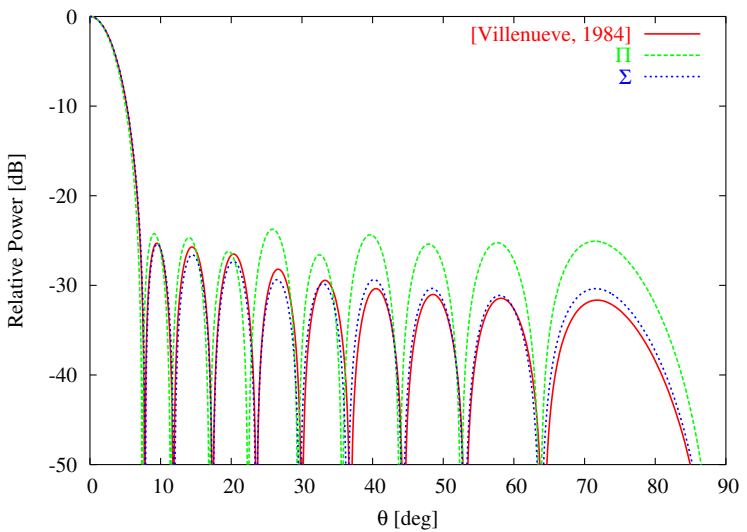
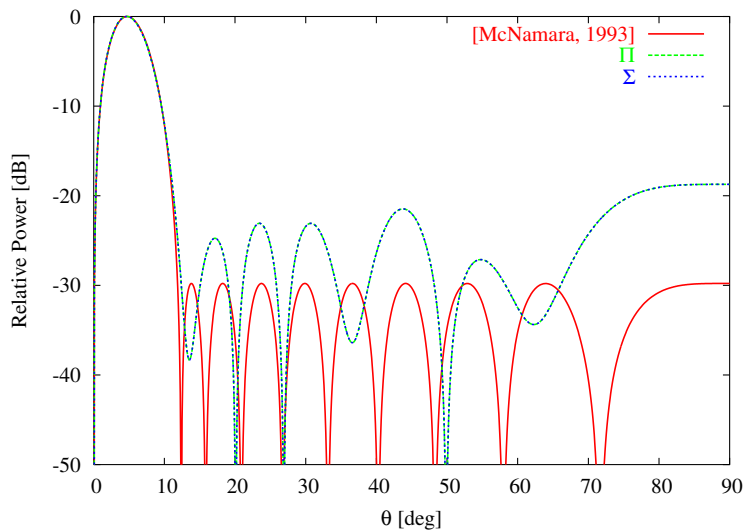


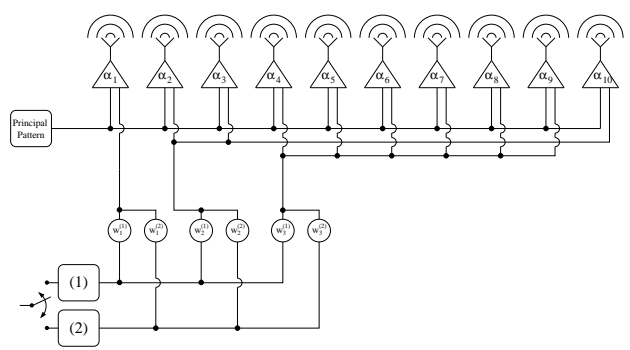
Fig. 5 - L. Manica *et al.*, “Synthesis of Multi-Beam Sub-Arrayed Antennas ...”



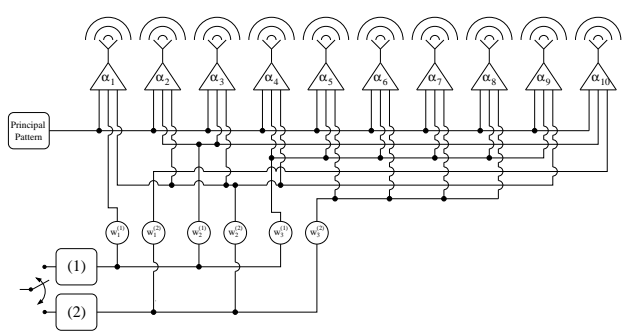
(c)



(a)

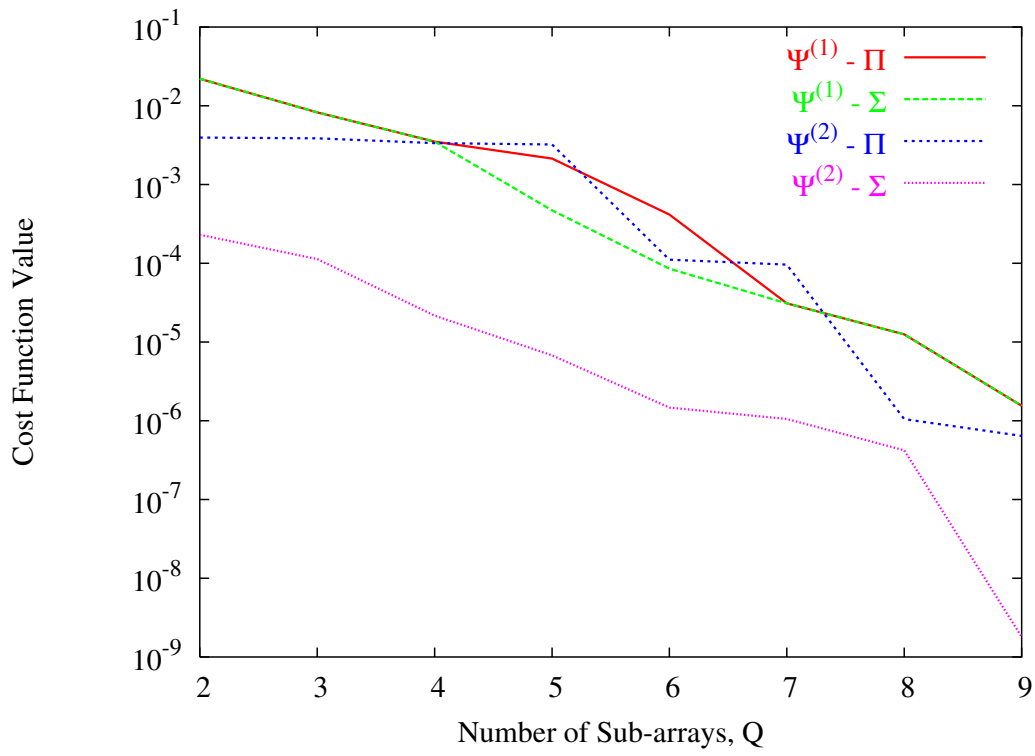


(d)

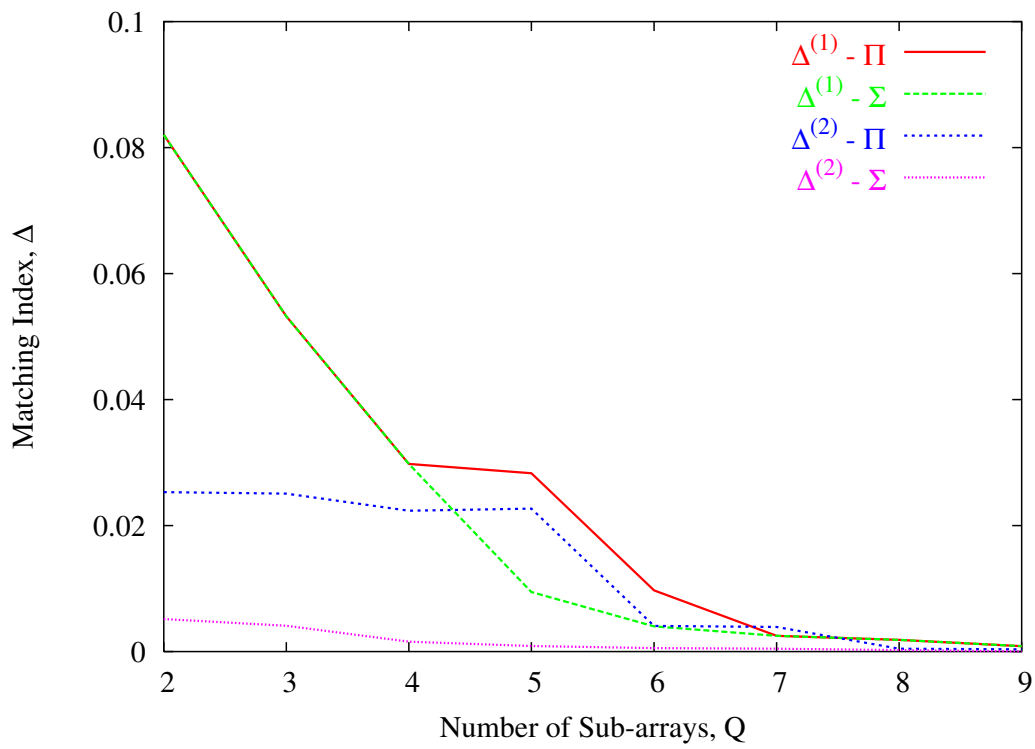


(b)

Fig. 6 - L. Manica *et al.*, "Synthesis of Multi-Beam Sub-Arrayed Antennas ..."

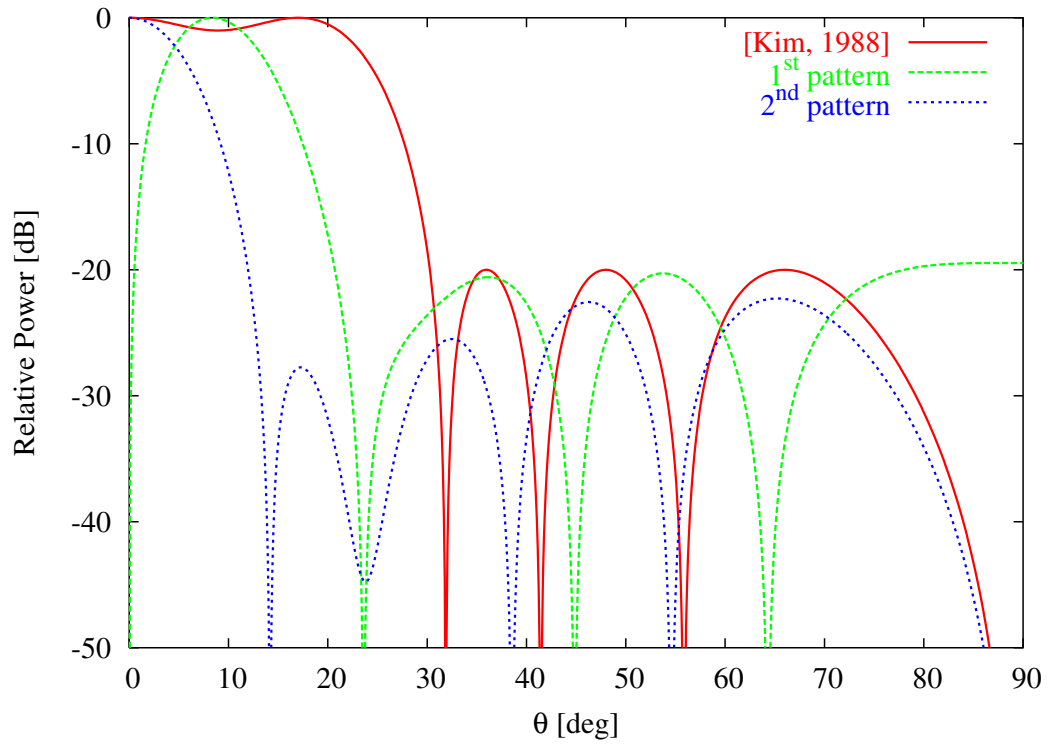


(a)

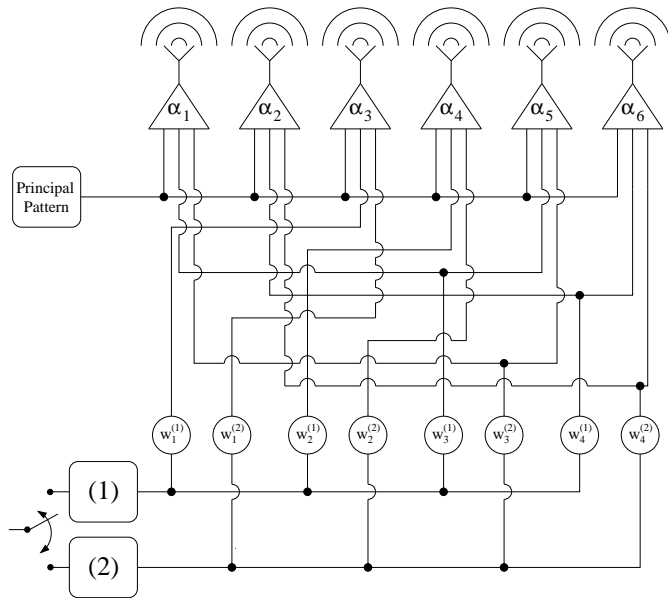


(b)

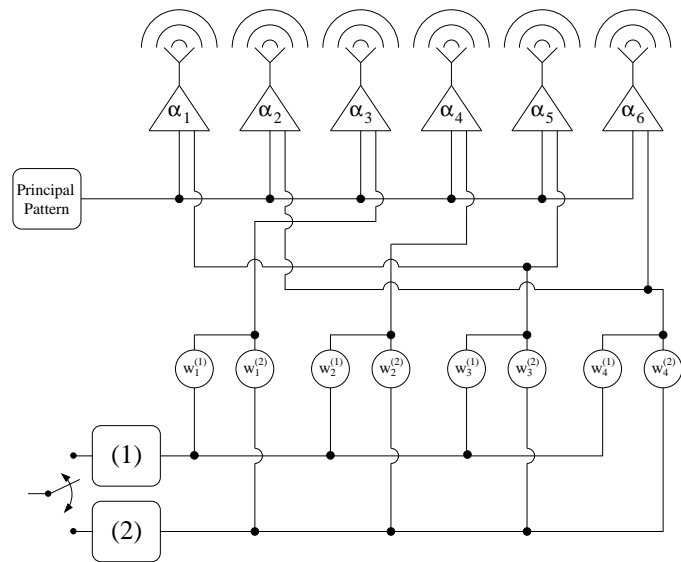
Fig. 7 - L. Manica et al., "Synthesis of Multi-Beam Sub-Arrayed Antennas ..."



(a)



(b)



(c)

Fig. 8 - L. Manica *et al.*, “Synthesis of Multi-Beam Sub-Arrayed Antennas ...”

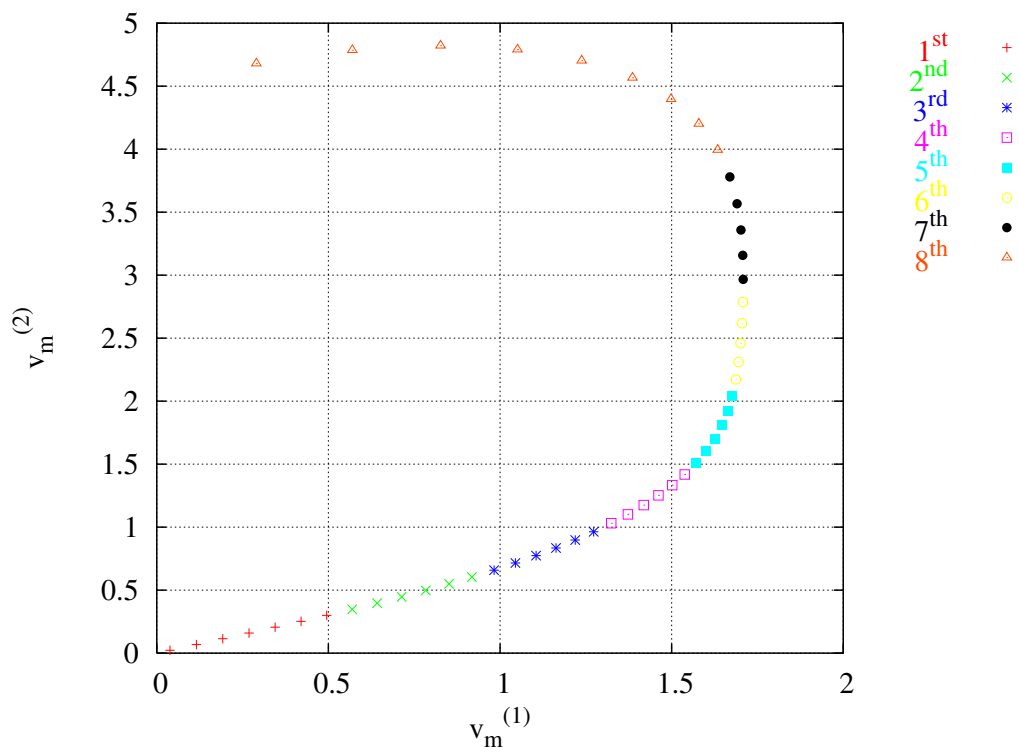


Fig. 9 - L. Manica *et al.*, “Synthesis of Multi-Beam Sub-Arrayed Antennas ...”

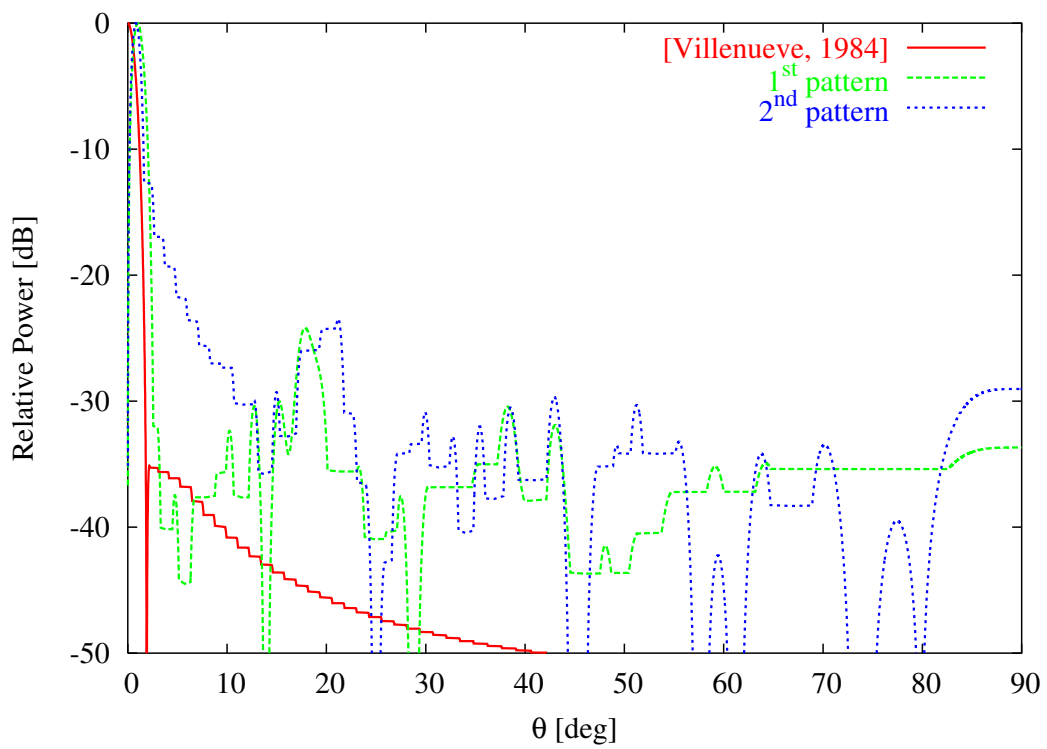
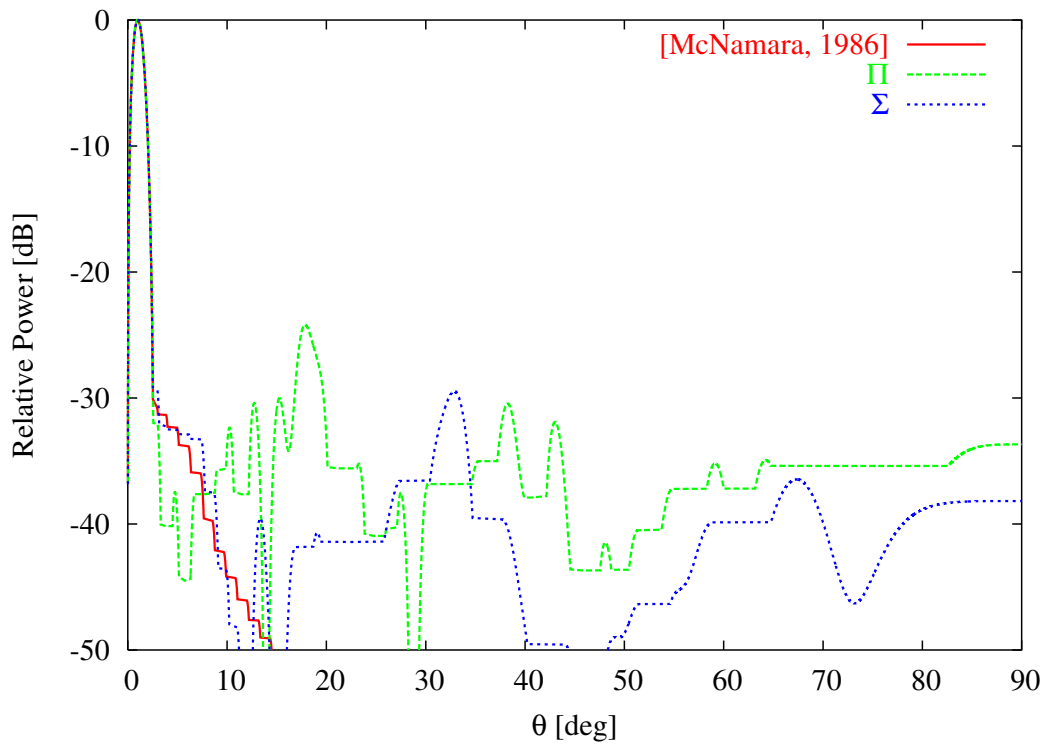
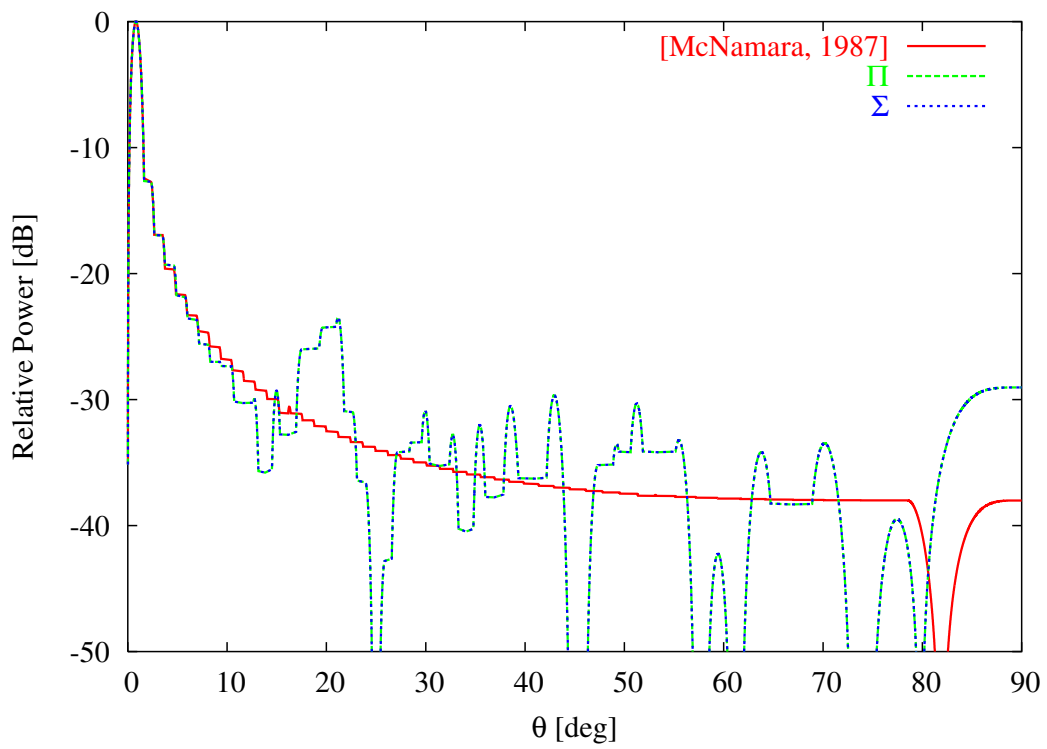


Fig. 10 - L. Manica *et al.*, "Synthesis of Multi-Beam Sub-Arrayed Antennas ..."



(a)



(b)

Fig. 11 - L. Manica *et al.*, "Synthesis of Multi-Beam Sub-Arrayed Antennas ..."

	\underline{V}_1	\underline{V}_2	\underline{V}_3	\underline{V}_4	\underline{V}_5	\underline{V}_6	\underline{V}_7	\underline{V}_8	\underline{V}_9	\underline{V}_{10}
$v_m^{(1)}$	0.1798	0.5275	0.8401	1.0973	1.2818	1.3818	1.3907	1.3074	1.1367	0.5742
$v_m^{(2)}$	1.0000	0.9998	0.9972	0.9896	0.9761	0.9609	0.9552	0.9811	1.0790	0.6397
r_m	1.0160	1.1304	1.3040	1.4776	1.6112	1.6831	1.6871	1.6346	1.5673	0.8586

Tab. I - L. Manica *et al.*, “Synthesis of Multi-Beam Sub-Arrayed Antennas ...”

$\Pi - Approach$			
\underline{C}	1 2 2 3 3 3 3 3 2		
$\underline{W}^{(1)}$	0.1798	0.6601	1.2549
$\underline{W}^{(2)}$	1.0000	0.9421	0.9807
$\Sigma - Approach - 1^{st} pattern$			
\underline{C}	1 2 2 3 3 3 3 3 2		
\underline{W}	0.1798	0.6601	1.2549
$\Sigma - Approach - 2^{nd} pattern$			
\underline{C}	2 2 2 2 3 3 3 3 2 1		
\underline{W}	0.6397	0.9682	1.0024

Tab. II - L. Manica *et al.*, “Synthesis of Multi-Beam Sub-Arrayed Antennas ...”

<i>Pattern (1)</i>	<i>BW [deg]</i>	θ_1 [deg]	<i>SLL [dB]</i>	$\Psi^{(1)}$	$\Delta^{(1)}$
$\Pi - Approach$	5.12	13.50	-18.73	0.8263×10^{-1}	0.5321×10^{-1}
$\Sigma - Approach$	5.12	13.50	-18.73	0.8263×10^{-1}	0.5321×10^{-1}
<i>Reference [8]</i>	5.15	12.42	-29.78	—	—
<i>Pattern (2)</i>	<i>BW [deg]</i>	θ_1 [deg]	<i>SLL [dB]</i>	$\Psi^{(2)}$	$\Delta^{(2)}$
$\Pi - Approach$	5.84	7.38	-23.73	0.3864×10^{-1}	0.2507×10^{-1}
$\Sigma - Approach$	6.08	7.83	-25.38	0.1129×10^{-2}	0.4083×10^{-2}
<i>Reference [6]</i>	6.06	7.74	-25.29	—	—

Tab. III - L. Manica *et al.*, “Synthesis of Multi-Beam Sub-Arrayed Antennas ...”

m	1	2	3	4	5	6
a_m [9]	1.0000	0.4577	-0.0838	-0.2033	-0.0278	0.1727
$\beta_m^{(1)}$ [8]	0.2847	0.7609	1.0000	0.9609	0.7135	0.4763
$\beta_m^{(2)}$ [4]	1.0000	0.9314	0.8051	0.6405	0.4615	0.4327
$v_m^{(1)}$	0.2847	1.6624	-11.9332	-4.7263	-25.6673	2.7578
$v_m^{(2)}$	1.0000	2.0350	-9.7064	-3.1504	-16.6001	2.5055
r_m	31.3575	33.0788	15.4121	24.8884	0.0000	34.2496

Tab. IV - L. Manica *et al.*, “Synthesis of Multi-Beam Sub-Arrayed Antennas ...”

<i>Pattern (1)</i>	<i>BW [deg]</i>	θ_1 [deg]	<i>SLL [dB]</i>	$\Psi^{(1)}$	$\Delta^{(1)}$
$\Pi - Approach$	9.29	23.58	-19.46	0.1626	0.5654×10^{-1}
$\Sigma - Approach$	9.29	23.58	-19.46	0.1626	0.5654×10^{-1}
<i>Reference [8]</i>	8.26	19.26	-24.51	—	—
<i>Pattern (2)</i>	<i>BW [deg]</i>	θ_1 [deg]	<i>SLL [dB]</i>	$\Psi^{(2)}$	$\Delta^{(2)}$
$\Pi - Approach$	10.59	14.22	-22.27	0.2385×10^{-1}	0.1624
$\Sigma - Approach$	10.59	14.22	-22.27	0.2385×10^{-1}	0.1624
<i>Reference [4]</i>	9.97	12.72	-24.76	—	—

Tab. V - L. Manica *et al.*, “Synthesis of Multi-Beam Sub-Arrayed Antennas ...”

$\Pi - Approach$								
\underline{C}	1111111222222333333444444555555666667777778888888888							
$\underline{W}^{(1)}$	0.2647	0.7403	1.1231	1.4276	1.6246	1.6978	1.6998	1.2174
$\underline{W}^{(2)}$	0.1584	0.4691	0.7983	1.2030	1.7361	2.4330	3.3103	4.4810
$\Sigma - Approach - 1^{st} pattern$								
\underline{C}	111112222233334444455556666677777888888888888888							
\underline{W}	0.1540	0.4566	0.7130	0.9473	1.1620	1.3440	1.5162	1.6659
$\Sigma - Approach - 2^{nd} pattern$								
\underline{C}	1111111222222333333444444555555666667777778888888888							
\underline{W}	0.1584	0.4691	0.7983	1.2030	1.7361	2.4330	3.3103	4.4810

Tab. VI - L. Manica *et al.*, “Synthesis of Multi-Beam Sub-Arrayed Antennas ...”

Tab. VII - L. Manica *et al.*, “Synthesis of Multi-Beam Sub-Arrayed Antennas ...”

<i>Pattern (1)</i>	<i>BW [deg]</i>	θ_1 [deg]	<i>SLL [dB]</i>	D_{max} [dB]	$\Psi^{(1)}$	$\Delta^{(1)}$
Π – Approach	1.09	2.67	–24.19	–17.05	0.7023×10^{-2}	0.1224×10^{-1}
Σ – Approach	1.10	2.67	–29.35	–17.05	0.1997×10^{-2}	0.6136×10^{-2}
Reference [33]	1.09	2.66	–30.72	–17.08	–	–
<i>Pattern (2)</i>	<i>BW [deg]</i>	θ_1 [deg]	<i>SLL [dB]</i>	D_{max} [dB]	$\Psi^{(2)}$	$\Delta^{(2)}$
Π – Approach	0.87	1.85	–12.71	–17.79	0.7023×10^{-2}	0.8230×10^{-2}
Σ – Approach	0.87	1.85	–12.71	–17.79	0.7023×10^{-2}	0.8230×10^{-2}
Reference [34]	0.86	1.85	–12.71	–17.84	–	–

	U	i_{opt}	ψ_{opt}	T [sec]
$\Pi - Approach$	1.4272×10^{45}	6	258	0.86
$\Sigma - Approach - Pattern (1)$	1.4272×10^{45}	11	125	0.08
$\Sigma - Approach - Pattern (2)$	1.4272×10^{45}	5	70	0.07

Tab. VIII - L. Manica *et al.*, “Synthesis of Multi-Beam Sub-Arrayed Antennas ...”